Using PSO algorithm for power flow management enhancement in PV-battery grid systems

Benslimane Abdelkader[1], Abdelhak Merabti[1], Benslimane Yamina[2]
[1]Department of Science Exact, Normal Higher School of Bechar, Bechar, Algeria
[2]Laboratory of Physics and Semiconductor Devices, Tahri Mohamed University, Bechar, Algeria

Article Info

Article history:

Received Oct 8, 2022
Revised Oct 30, 2022
Accepted Nov 13, 2022

Keywords:

Battery storage system
DC/DC bidirectional converter
Fuzzy logic
PSO
PV Solar

ABSTRACT

In this article, we have shown the possibility of improving the quality of the energy injected into the electrical network and the flexibility of its exchange between the different components of the proposed hybrid network (photovoltaic generator connected to the network-storage battery-load of the DC motor) to develop a control element based on the combination of fuzzy logic and an algorithm derived from PSO Animal Behavior. The proposed control works on DC/AC and bi-directional DC/DC converters, which form the basis of power management between the parts of the proposed hybrid network. MATLAB/Simulink software is used to demonstrate the effectiveness of the proposed control. The results show that the proposed control contributed to the stability of the photovoltaic energy produced, the improvement of the quality of energy injected into the network, as well as the response speed during the process of charging and discharging the battery, which gave more efficiency to the DC motor connected to the DC bus.

Corresponding Author:

Benslimane Abdelkader
Departement of Sience Exact, Normal Higher School of Bechar
ENS Elbarga, Bechar County 08001, Algeria
Email: slimane_kada@yahoo.fr

1. INTRODUCTION

The problems caused by the use of fossil fuels, such as climate change, the shortage of production and the increase in prices, are among the most important reasons which have led to the trend towards renewable energies (solar and wind). In [1], [2] advances in technology especially in the field of power electronics and the evolution of the PV market over the last decade have contributed to giving a kind of reliability to photovoltaic energy.

Furthermore, the development of intelligent regulation in the PV industry has facilitated the quick advancement of PV applications, particularly PV systems connected to the energy grid, which have increased in size from a few kW to over 100 MW [3], [4]. To do this, the photovoltaic system's converters must perform better in order to raise the system's efficiency. By suggesting an inverter control scheme with a boost chopper to connect the grid to the PV generator, which delivers optimal PV power and high-quality current injected into the grid, this work contributes to improving the efficiency of the PV-battery-grid connected inverter DC/AC. In the literature, various control techniques have been considered, like [5], an intelligent algorithm based on direct current and DC link voltage controllers for a three-phase grid-connected photovoltaic inverter is presented in this work. Lakshmi and Hemamalini [6] presented a unique approach for the global maximum photovoltaic power generated (MPPT) controller is put forth that solves the PSC shading problem by applying the moth-flame (MFO) optimization technique. Farhat *et al*. [7] suggested to use a fractional proportional-integral (FO-PI) controller to decouple control of a grid-connected PV system. According to the power produced by the solar systems and the power consumed by the electrical network, this decoupled control method enables separate control of the actual power (P) and the reactive power (Q). Aatif *et al*. [8] presented a PI-GA controller was used to improve the performance of a 3-phase grid-connected PV system by adjusting the K_P and K_i values of the PI controller of the current regulator that was used to control the P and Q powers of the system . In this paper, the FLC tuned by PSO is introduced into two regulation loops. The first is the DC voltage regulation loop for the DC/AC inverter control, and the second is the battery charge/discharge current regulation loop for the buck-boost bidirectional converter control. The goal is to improve the stability and efficiency of the system and improve the quality of energy injected into the grid. In addition to that, we used the fuzzy logic controller to extract the MPPT of a PV generator surrounded by volatile weather conditions. Therefore, a comparative study of two methods (PI and PI-FLC PSO) has been proposed, which will be covered in more detail in the sections that follow. MATLAB/Simulink will be used to run the simulation.

2. SYSTEM DESCRIPTION

The proposed controller inverter DC-AC (CIDA) is responsible for ensuring flexibility in energy exchange between the DC source (GPV-storage battery) and the grid connexon via the HB bridge three-phase inverter DC/AC with boost converter that is used to extract the MPPT. The configuration of the PV system chosen in this study is shown in Figure 1. The power of the PVG is equal to 286 kW with a capacity battery of 1500 A/h. The existence of a bidirectional converter (BUCK-Boost DC/DC) is necessary to interconnect the battery with the other equipment of the system. Because of its dual functionality, it functions as a boost converter in charge mode and a buck converter in discharge mode [8] , [9].

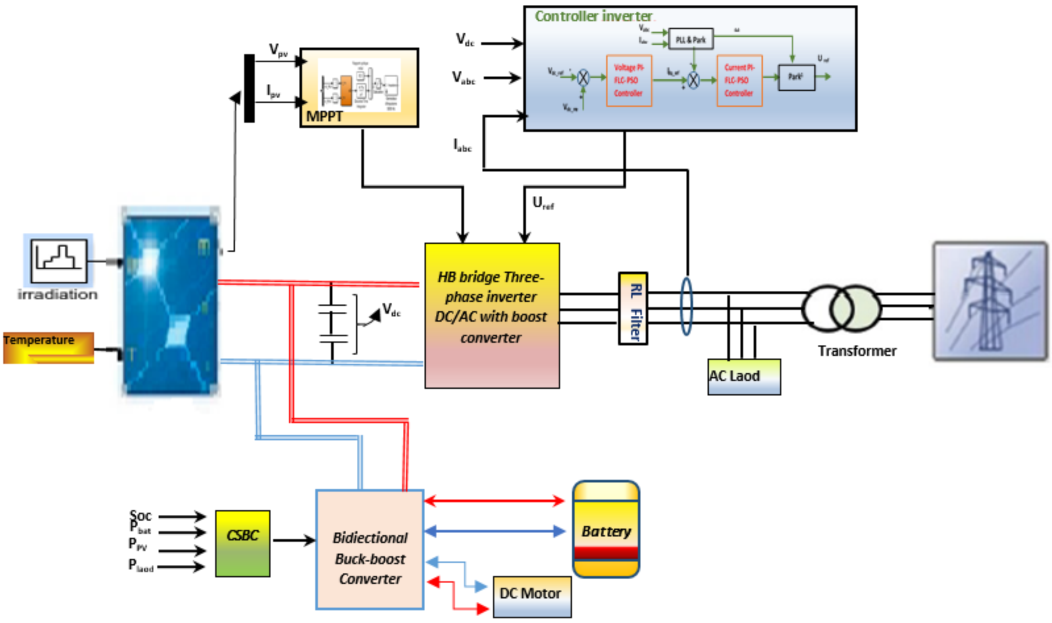

Figure 1. Studied PV system (100 kW)

2.1. PV generator (PVG)

The mathematical model of PVG is deduced from the mono-diode model of the PV cell. It is given by (1) [10], [7]. Figure 2 shows the (I-V) characteristics of the PVG used in the simulation.

$$I = N_p I_{PV} - N_p I_0 \left(e^{\left(q\left(V + R_S \frac{I N_S}{N_p}\right)/A\,k\,T N_S\right)} - 1\right) - \frac{V + (R_S I N_S/N_p)}{R_p + (N_S/N_p)} \quad (1)$$

2.2. Three-phase inverter (TPI) DC/AC

As shown in Figure 3 the inverter has three independent inputs, each consisting of a filter that eliminates electromagnetic interference and a boost chopper (only a single input is indicated in Figure 3) [11]–[13]. The three Boost converters are connected in parallel on a three-phase bridge (3 half bridges), which then converts the direct current (DC) supplied by the DC/DC converter into alternating current (AC) using the PWM technique, the fundamental of which is at the frequency of 50 Hz [14], [15]. The midpoint (B) of the capacitors is located just before the three-phase bridge is connected to the network neutral. A filter eliminates high frequency harmonics to obtain a sine wave [16], [17]. The operation of this inverter requires that the switches of the same arm not be simultaneously blocked, and Table 1 shows the eight possible operating states of the TPI switches (K_1, K_2,..K_6) shown in Figure 3 [5], [18].

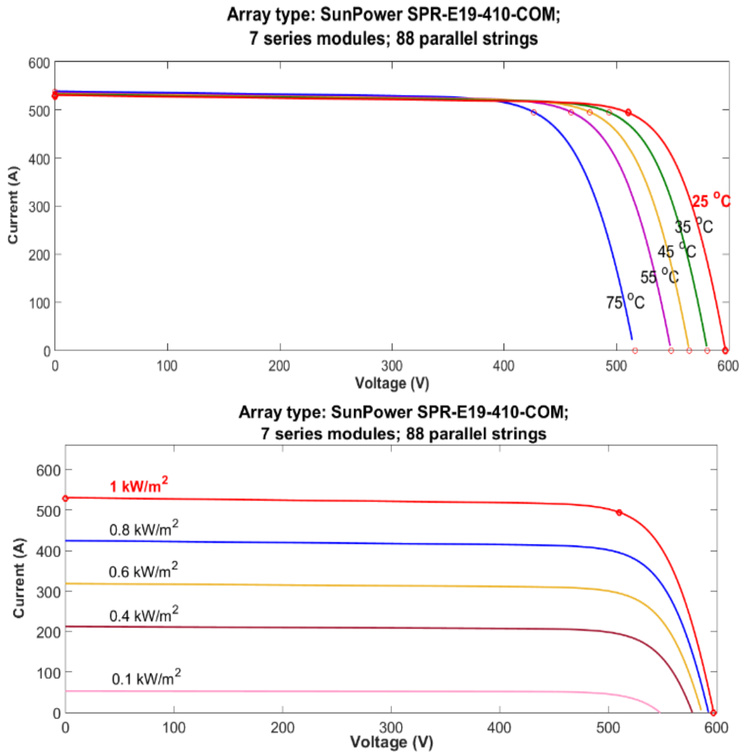

Figure 2. (I-V) characteristic curves for different values of (irradiance and temperature)

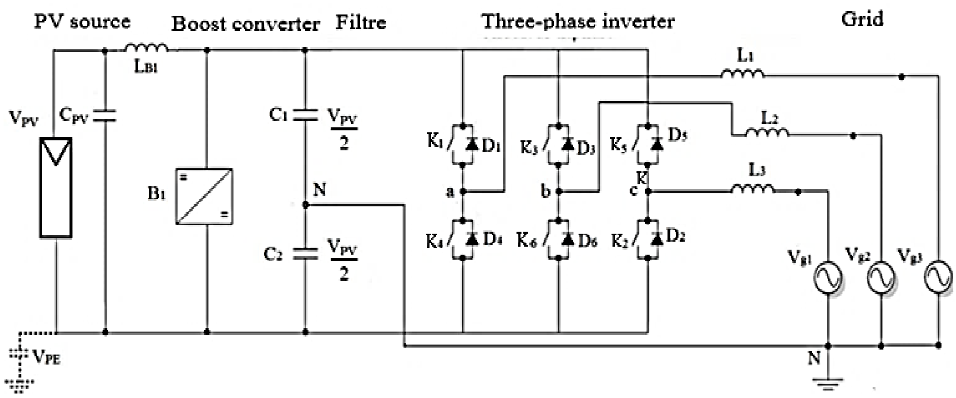

Figure 3. HB bridge TPI DC/AC with boost converter

Table 1. Operating states for a TPI

State	Vab	Vb	Va	Space vector
(K_1, K_2, K_6) conduct and (K_3, K_4, K_5) are blocked	V	0	-V	V_1 = 1+0,5j
(K_1, K_2, K_3) conduct and (K_6, K_4, K_5) are blocked	0	V	-V	V_2 =1,155j
(K_2, K_3, K_4) conduct and (K_1, K_6, K_5) are blocked	-V	V	0	V_3 =1+0,5j
(K_3, K_4, K_5) conduct and (K_1, K_2, K_6) are blocked	-V	0	V	V_4 =1-0,5j
(K_4, K_5, K_6) conduct and (K_1, K_2, K_3) are blocked	0	-V	V	V_5 = -1,155j
(K_1, K_5, K_6) conduct and (K_3, K_4, K_2) are blocked	V	-V	0	V_6 = 1-0,5j
(K_1, K_3, K_5) conduct and (K_2, K_4, K_6) are blocked	0	0	0	V_7 = 0
(K_4, K_2, K_6) conduct and (K_3, K_1, K_5) are blocked	0	0	0	V_8 = 0

2.3. Bidirectional DC-DC converter (BDC)

The buck-boost converter shown in Figure 4. Combines two properties: increasing and decreasing DC voltage to convert [19], [20]. The BDC's potential operating scenarios are shown in Table 2.

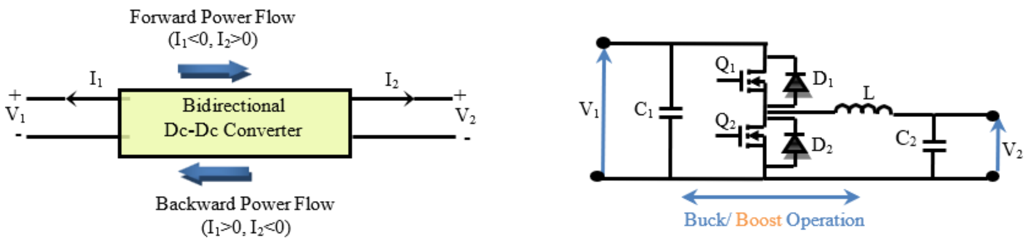

Figure 4. The circuit diagram of the BDC

Table 2. The various BDC operational scenarios

Case	Swith/ dioc	State of swith and diode	Power flowing direction	Voltage comparison	Bidirectional mode	State of battery
1	Q1	ON	Forward	V_{in}=V_1(high voltage side)>V_{out}=V_2(low voltage-side)	Buck	Charging
	Q2	OFF				
	D2	Active				
2	Q1	OFF	Backward	V_{in}=V_2(low voltage side)<V_{out}=V_2(high-voltage side)	Boost	discharging
	Q2	ON				
	D1	Active				

2.4. Battery system

Figure 5 shows the equivalent circuit and the battery discharge characteristics (nickel-metal hybrid) used in the simulation. This work was carried out using the implementation of a parameterized dynamic model to represent this type of rechargeable battery. This type of battery is used in [21]. The relationship between the parameters is noted in (2).

$$A.h_{used} = A.h \times \left(1 - SoC_{(0)}\right) + \int \left(\frac{\left((V_{oc} - \sqrt{4R_{int} - P_{el}/2R_{int}}\right)}{3600}\right) dt \tag{2}$$

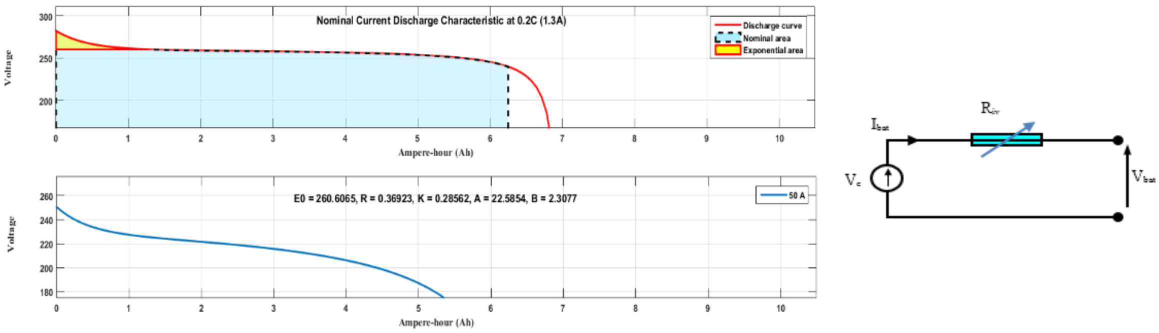

Figure 5. Plot charging/discharging battery and equivalent circuit

2.5. DC motor load

The Figure 6 illustrates the analog DC load circuit and their associated equations that connect the various parameters. the solution of these coupled differential equitation is difficult in this form. But when we apply the Laplace transform for these equations become there algebraic and the system linear [16].

$$\begin{pmatrix} v_{DCch} = e + R_a i_{ch} + L_a \frac{di_{ch}}{dt} = e + R_a i_{ch} \\ e = K_b \omega_m \\ P_{el-DC-ch} = v_{DCch} i_{ch} = e i_{ch} + R_a i_{ch}^2 \end{pmatrix} \tag{3}$$

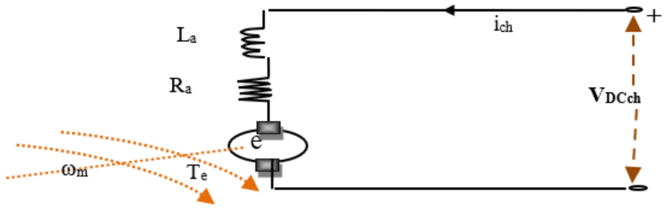

Figure 6. Modeling of a DC motor

3. SYSTEM CONTROL

3.1. Control strategy for the TPI DC/AC control

The architecture of the DC/AC controller is shown in Figure 7. It is based on two regulation loops, one for optimal regulation of the intermediate circuit voltage and the other for external control of the direct and quadrature currents (Id, Iq) given by the phase-locked loop. For the PVG to work in PPM, it is mandatory to have an MPPT command that acts on the converter boost incorporated into the TPI. In addition, a bidirectional buck-boost converter ensures both battery operation (charge/discharge) and motor power supply thanks to the existence of an energy management control (CSBD) [21].

In general, control loops mainly depend on PI controllers. Our goal in this work, is to wait for an optimal gain, that's why we replaced these controllers with others based on fuzzy logic and the meta-heuristic algorithm, which calls for particle swarm optimization (FLC–PSO) for the purpose of improving the dynamic performance of the proposed system.

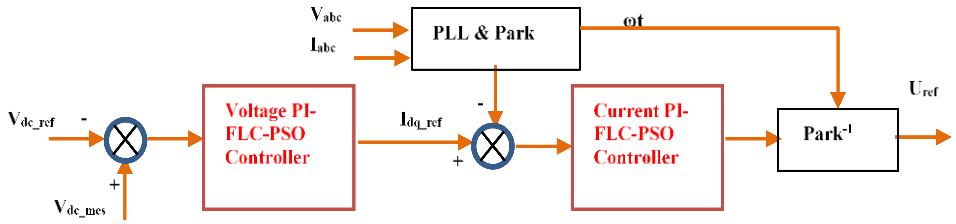

Figure 7. Control inverter DC/AC

3.2. Control approach for CSBC

To maximise efficiency, maintain the continuity of the power supply and manage the exchange of power flows with better stability, we have adopted in this work a bidirectional converter control strategy (CSBC) optimised by the PSO algorithm [22], [23]. This strategy is shown in Figure 8.

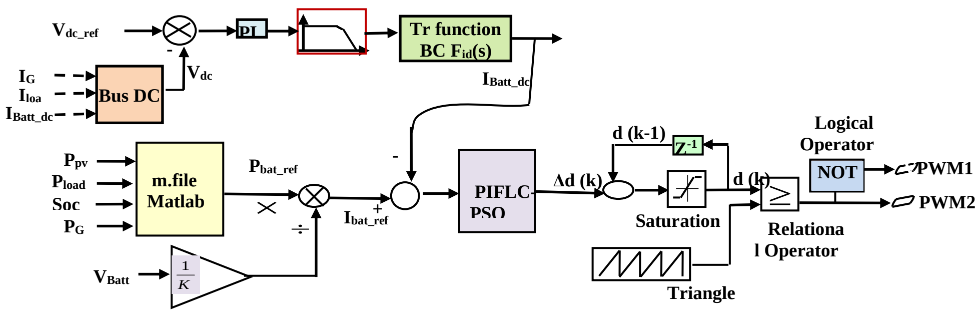

Figure 8. Structure of SCBC

3.3. PIFLC-PSO controller

In this work, we've proposed a method for adjusting the scaling factors for the PI-type FLC controller based on the PSO algorithm, which is applied in two control loops (current & DC link) of the DC/AC inverter as shown in Figure 9. This tuning technique was put out in references [24], [25].

$$u_c = \beta \int u\, dt = \beta \int (A + Pk_1 e + Dk_2 e^{'})dt = \beta At + \beta k_2 De + \beta k_e P \int e\, dt \quad (4)$$

By (4), the FLC transforms into a time-varying PI controller, and its proportional equivalents, the control and integral control components, are, respectively, $\beta k_2 D$ and $\beta k_2 D$ The term "PI-FLC" refers to this fuzzy controller [26], [27].

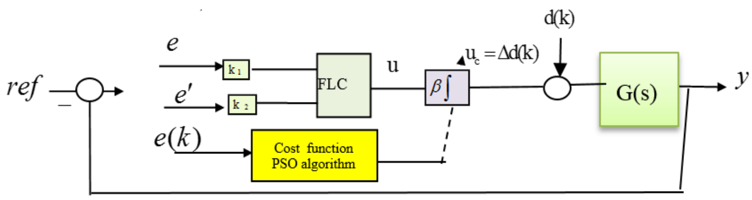

Figure 9. Block diagram for the PIFLC-PSO controller

Practically speaking, the Fuzzy PI type of control is better at suppressing steady-state mistakes. However, because of the internal integration process, it performs poorly in the transitory response to the higher order process. Performance is enhanced by coupling a serial integrator to the PI-type fuzzy controller's output, whose inputs include errors and error rate of change. Figure 8 shows a block diagram in which fuzzy variables are multiplied by scaling factors (k1, K2) before being applied to the fuzzy block and fuzzy output variables in (5), with the adjustment of the output scaling factor β is performed using a PSO algorithm [27], [28].

$$\begin{cases} E(k) = k_1 e(k) \\ \Delta E(k) = k_2 ((\frac{e(k)-e(k-1))}{T}) \\ d(k) = d(k-1) + \beta . k_1 \Delta d(k) \\ e(k) = (e_{inverter(DC/AC)1}[k]); or (e_{inverter(DC/AC)2}[k]); or (e_{biderectional(DC/DC)}[k]) \end{cases} \quad (5)$$

Figures 10(a) and 10(b) display the surface maps (input and output) of the controllers (FLC-CSBC) and (FLC-TPI DC/AC) accomplished using a Mamdani fuzzy inference method. The technique of iteratively minimizing a cost function to estimate the ideal variables was done using the PSO algorithm, which scaled the output factor (β). In (6) and (7) shows, respectively, the formula for the continuous (J_c) and discontinuous (J_d) temporal performance indices.

$$\begin{cases} J_c = k \int |e(t)|\, dt \\ e_{inverter(DC/AC)1}(t) = V_{dc\_ref} - V_{dc\_mes}(t) \\ e_{inverter(DC/AC)2}(t) = I_{dq\_ref} - I_{dq\_meas}(t) \\ e_{Bidireactional(DC/DC)}(t) = I_{batt\_ref} - I_{batt\_mes}(t) \\ t \in [0, t_1] \end{cases} \quad (6)$$

$$\begin{cases} J_d = k \sum_{i=1}^{k} |e(i)| \\ e_{inverter(DC/AC)1}[k] = V_{dc\_ref} - V_{dc\_mes}[k] \\ e_{inverter(DC/AC)2}[k] = I_{dq\_ref} - I_{dq\_meas}[k] \\ e_{Bidireactional(DC/DC)}[k] = I_{batt\_ref} - I_{batt\_mes}[k] \\ k = 1,2, \dots, itermax \end{cases} \quad (7)$$

– Using PSO algorithm for scaling β

The optimization of these scale factors is suggested as a potential remedy to cope with challenges and errors in selecting appropriate values for the scale factors of each PID type FLC structure by the test processes. Chettibi and Mellit [21] using PSO optimization, we were able to determine the best choice variables $x^* = (k_1^*, k_2^*, \beta^*)^T$ to represent the scale factors of a certain FLC structure that is similar to a PID and minimises the desired cost function based on the maximum overshoot (MO) and integral of absolute error (IAE) performance criteria (IAE). Overshoot D, steady state error E_{ss}, rise time t_r and settling time t_s of the system step response are among the time domain control requirements shown in (8), which also include other needs.

$$\begin{cases} \min; f(x)_{;x=(k_1,k_2\,\beta)^T \in R^3} \\ subject\ \ to \\ D \le D^{max}\ ;\ t_s \le t_s^{max}\ ;\ t_r \le t_r^{max}\ ; E_{ss} \le E_{ss}^{max} \end{cases} \tag{8}$$

Where *f* denotes the cost function.

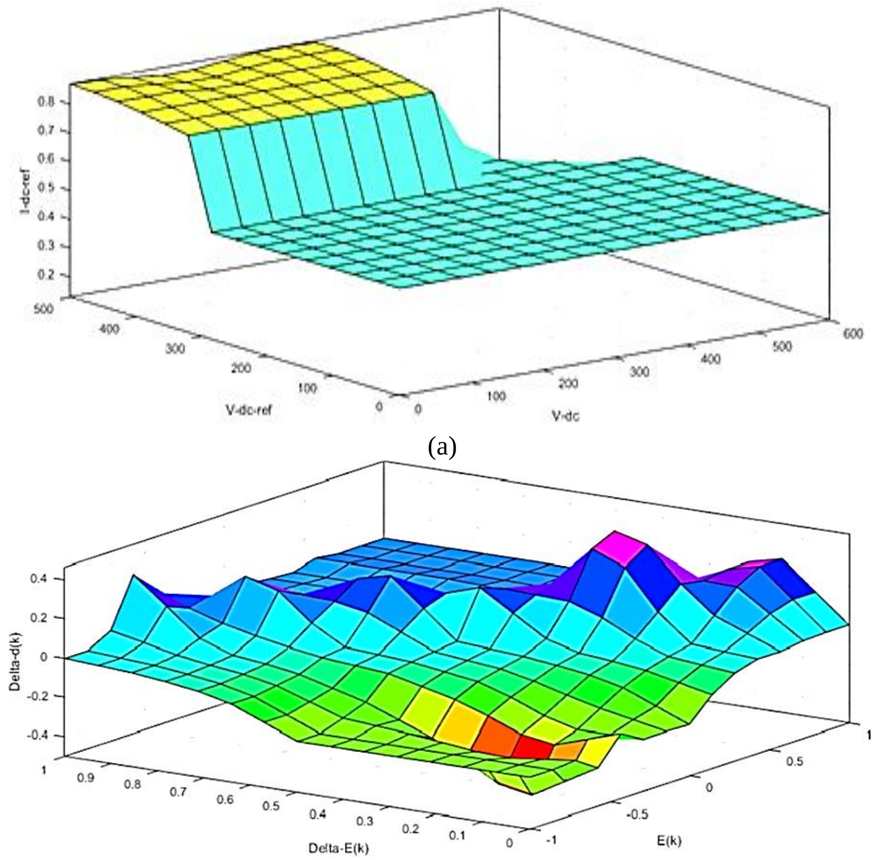

Figure 10. Surface input/output: (a) FLC-CSBC and (b) FLC-TPI DC/AC

PSO is a meta-heuristic algorithm that draws inspiration from migrating bird behaviour. We attribute the construction of artificial intelligence [29]. The (9) and (10) show the standard formulations of PSO commonly used.

$$\left(\begin{array}{c} x_i^{(k+1)} = x_i^{(k)} + v_i^{(k+1)} \\ v_i^{(k+1)} = w(k) \cdot v_i^{(k)} + c_1 \cdot r \cdot \left(x_{pbest}^k - x_i^{(k)}\right) + c_2 \cdot r \cdot \left(x_{gbest}^k - x_i^{(k)}\right) \\ k = 1, 2, 3, \dots \dots \dots, n \end{array} \right. \tag{9}$$

$$\left(\begin{array}{c} w(k) = w_{max} - (\frac{w_{max} - w_{min}}{k_{max}}) \\ F_1(k) = \sum_{i=1}^{N} \left| e_{inverter(DC-AC)1}(i) \right| \\ F_1(k) = \sum_{i=1}^{N} \left| e_{inverter(DC-AC)2}(i) \right| \\ F_1(k) = \sum_{i=1}^{N} \left| e_{biderectional(DC-DC)}(i) \right| \end{array} \right. \tag{10}$$

Where: x_i^k : the i_{th} p article's position; v_i^k : i_{th} particle velocity; p_{best} : person's ideal place; k : Number of iterations; G_{best} : best position attained by the swarm's particles; w : Inertia term is calculated by (10); $F_{1,2,3}(k)$: Fitness function; $0 \le r \le 1$.

$$c_1 = c_2 = 2.05;\ w_{min} = 0.4;\ w_{max} = 0.9; N = 30$$

The fundamental elements of the algorithm are:
Set the starting random elements. p_{best}, g_{best}, xp_{best} and xg_{best}
For each iteration *k;*
Update *w* by applying (10);
For each particle i of the population;
Update V_i^k and X_i^k of all particle at iteration k using (9);
Evaluate the fitness of all particles
If fitness (x (i)) < p_{best}(i) then update xp_{best} and p_{best}
xp_{best} = x (i); p_{best} = fitness (x (i));
If p_{best}< g_{best} then update xg_{best} and g_{best}
xg_{best} = xp_{best}; g_{best}= p_{best};
Next particle; Next iteration
xg_{best} is the solution

4. RESULTS AND DISCUSSION

The grid-connected PV system is depicted in Figure 11 and is developed in MATLAB/Simulink. It consists of the PV generator, HB bridge three-phase inverter DC/AC with boost converter, the bidirectional converter, storage battery, and DC load motor. In this study, we compared the effectiveness of conventional control to intelligent control (PIFLC-PSO), which depended on the PSO algorithm, in terms of how well the solar generator performed and how well the battery was charged and discharged. It was also determined how much of an improvement in energy quality the DC/AC inverter that was installed on the grid had made.

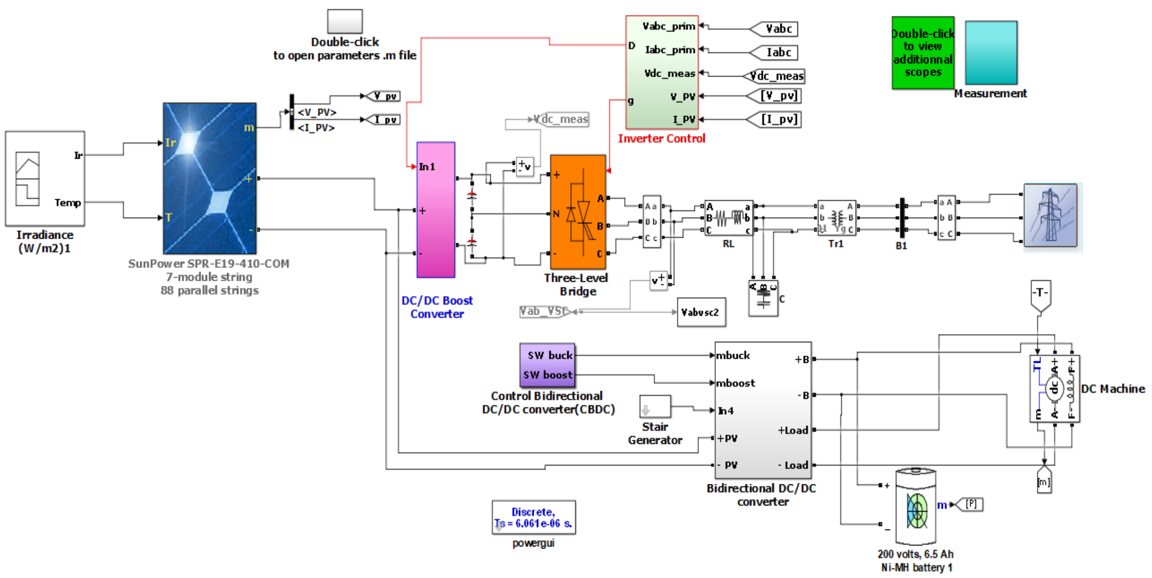

Figure 11. Model configuration in Simulink

In this simulation, the solar radiation is randomly varied between 200 and 1000 w/m² as shown in Figure 12. The output voltage from the DC/AC Boost HB Bridge Three-phase inverter DC/AC that connects the PV generator to the grid has been shown in Figure 13. The change in illumination leads to the change in alternating current produced by the TPI-DC/AC converter.

Compared to the traditional regulator (PI), the adoption of the intelligent regulator (PI-FLC-PSO) increases the stability of the photovoltaic power delivered. This is evident by zooming into the interval [0.95-1] in Figure 14. The comparative evaluation of the Soc Battery presented by Figure 15 demonstrates the lowest Soc value in the (PI-FLC-PSO) control increased by 0.013% compared to the other cases (PI and PI- FLC), considering the identical circumstances for the suggested system.

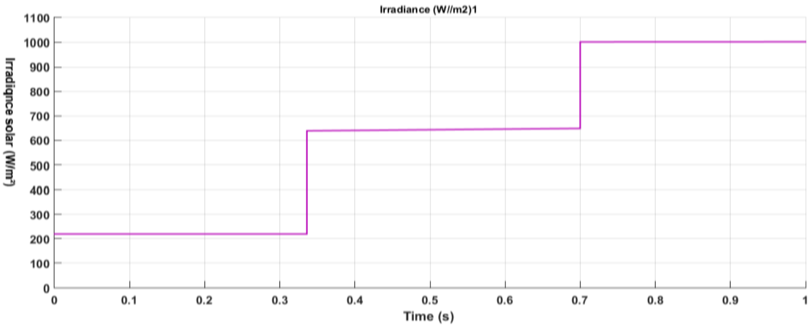

Figure 12. Irradiance solar

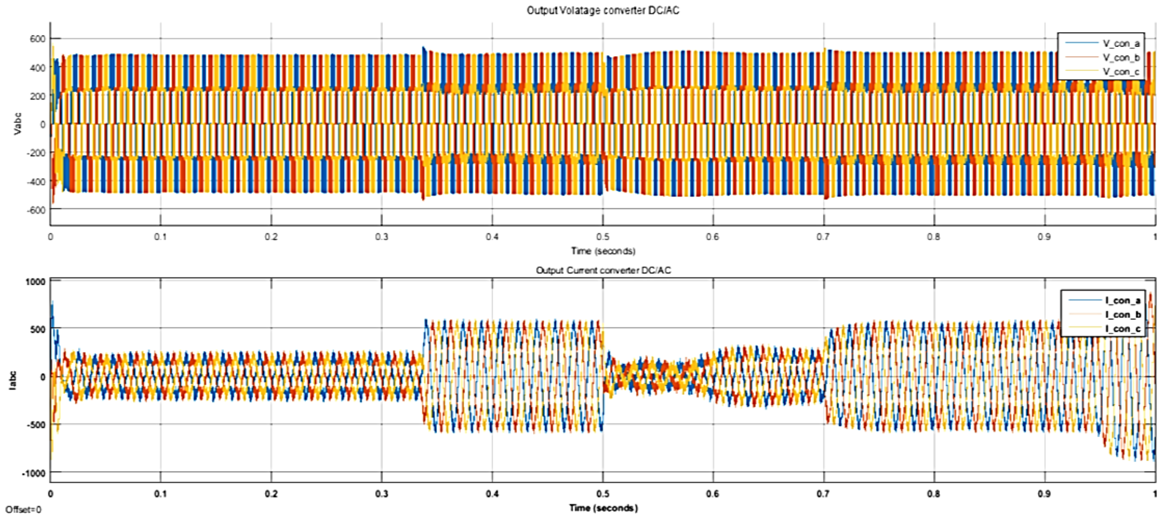

Figure 13. Output voltage and current DC-AC converter

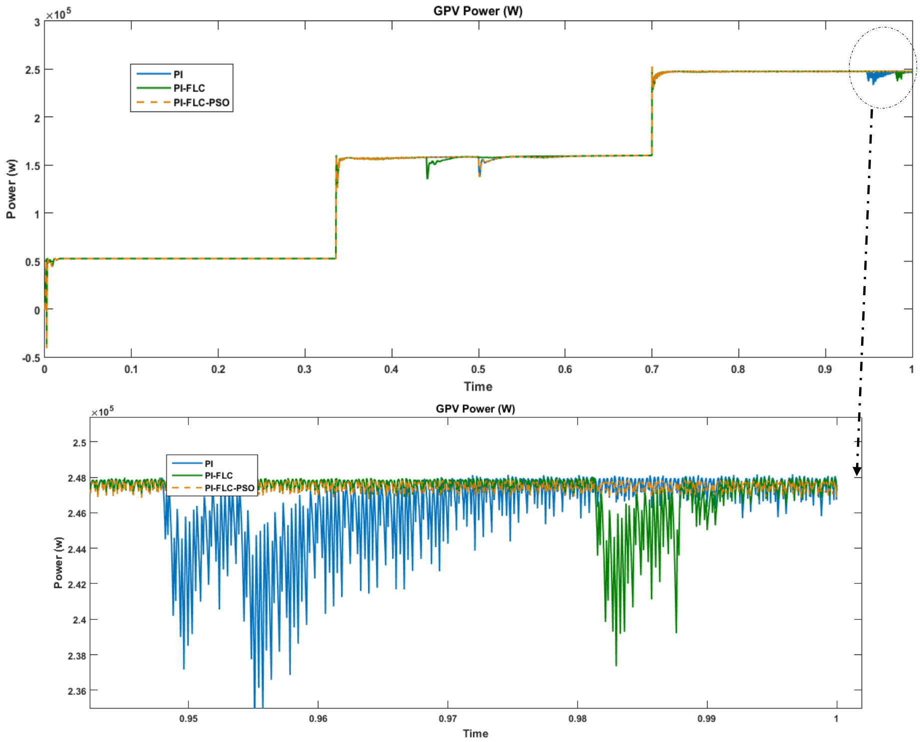

Figure 14. Output GPV power

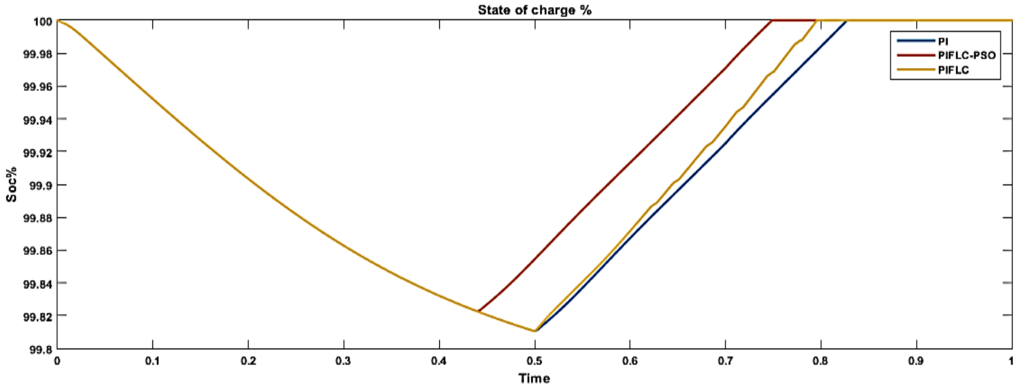

Figure 15. State of charge battery (SOS%)

Comparing the DC motor speed curve of the three control scenarios (PI, PI-FLC, and PI-FLC-PSO) is illustrate in Figure 16 reveals improved response time and stability when using a PI-FLC controller adjusted by the PSO algorithm. There is a 0.5-second gap between them. Figures 17 and 18 present the harmonic distortion rates of the voltages injected by the inverter to the connection transformer with the network and that of the network voltage in the three cases of the regulation (PI; PIFLC; PIFLC-PSO). In the case of the use of a PI-FLC-PSO, an improvement in the THD% of the order of (0.4%-0.34%=0.06%) for the voltage injected by the inverter and of (56.68%-46.65%=10.03%) for mains voltage was noticed.

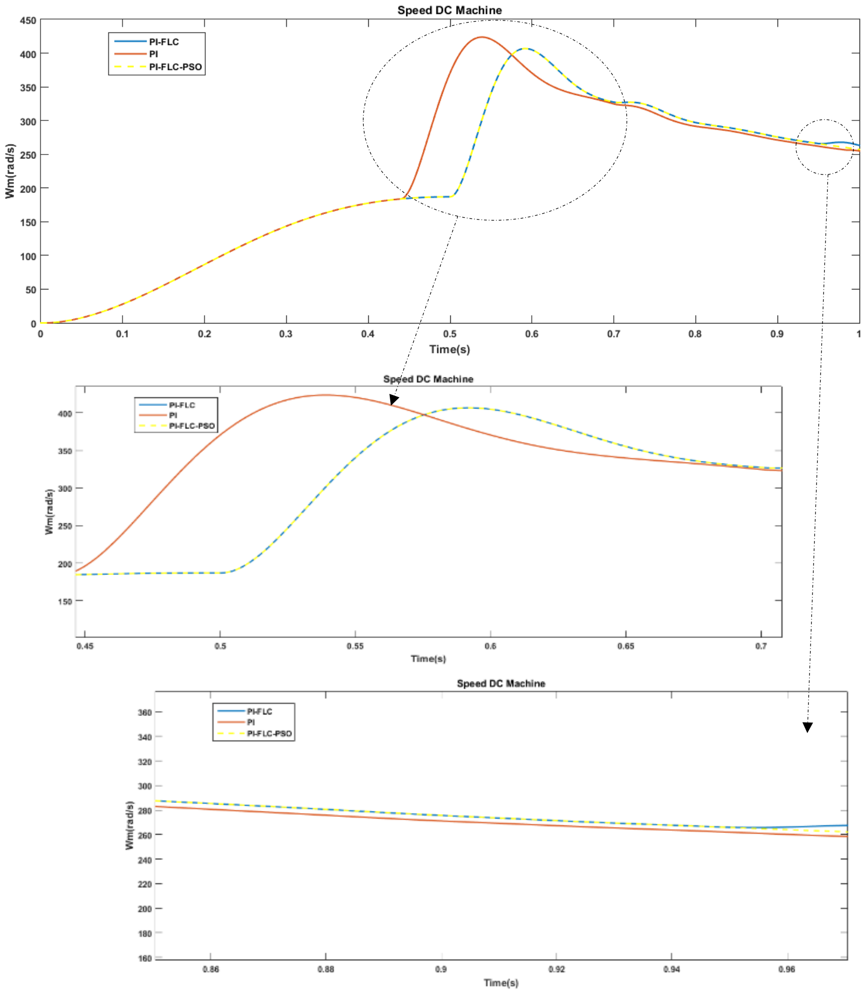

Figure 16. Speed DC motor load

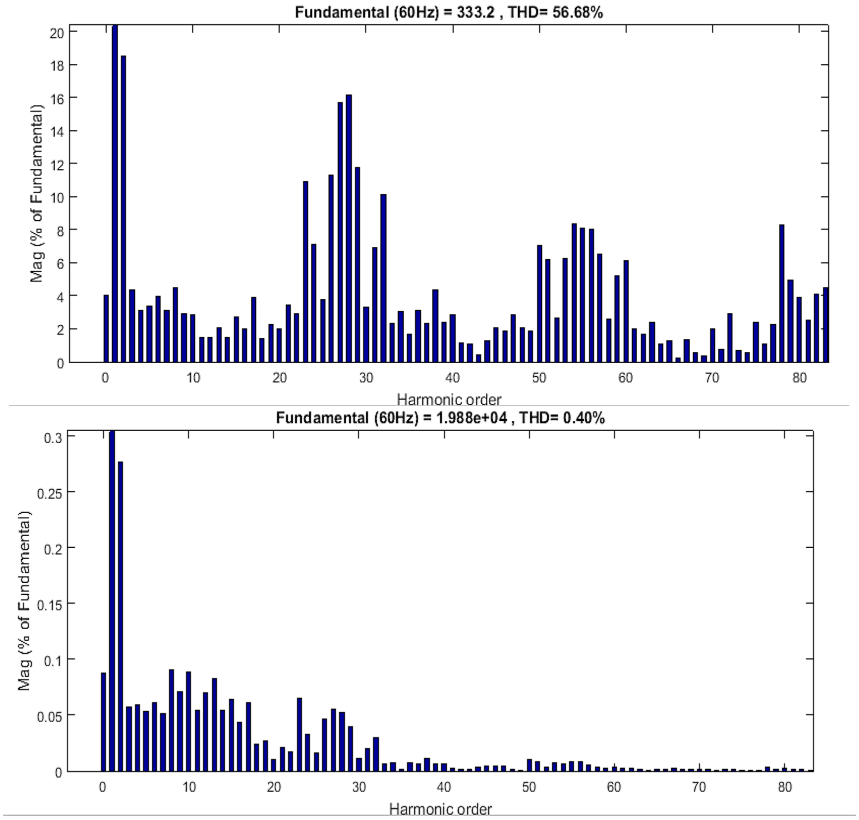

Figure 17. THD% [tension DA/AC converter and grid case (PI-PIFLC)]

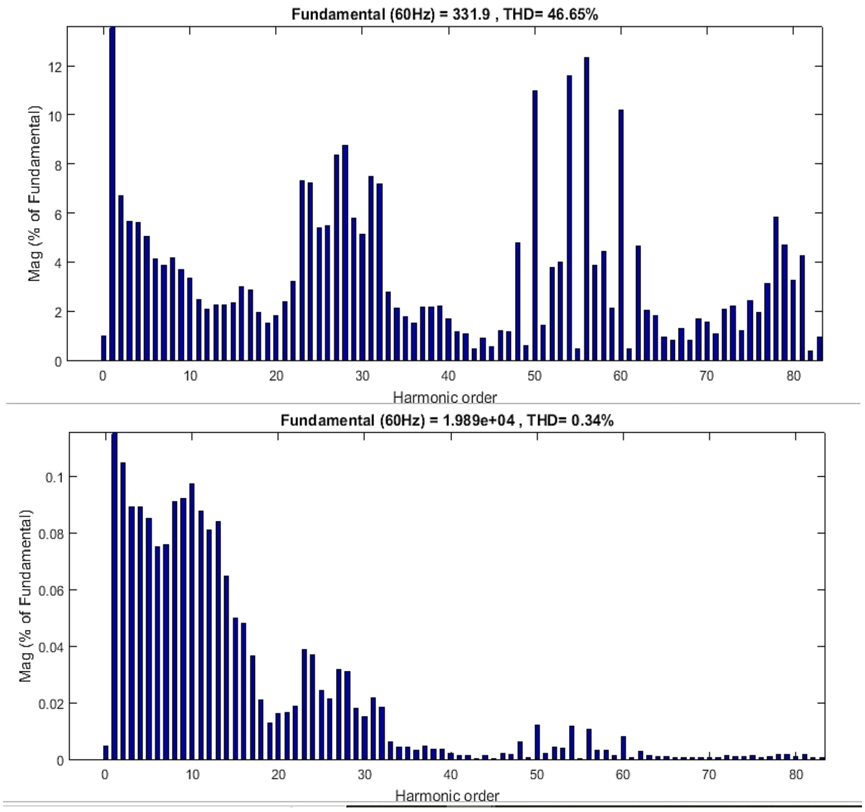

Figure 18. THD% [tension DA/AC converter and grid case (PIFLC-PSO)]

5. CONCLUSION

An intelligent control strategy-based PIFLC adjusted by PSO has been introduced in the regulation of DC-AC Inverters and DC-DC bidirectional converters to improve the quality of energy injected into the network on the one hand and better manage the flow of energy between the different parts of the system (GPV-battery storage) grid-connected on the other hand. This change in regulation strategy is implemented and evaluated in the MATLAB/Simulink environment. First, the influence of the PIFLC-PSO controller on the external DC coupling voltage control loops and the direct current and internal quadrature control (Id, Iq) provided by the PLL of the DC/AC inverter is remarkable, according to the simulation results, which reveal that the PIFLC-PSO provides the best THD values. Secondly, the calculation of the optimal values of the PIFLC controller output scale factor of the battery charge/discharge current control loop of the bidirectional DC/DC converter by the PSO algorithm makes it possible to ensure an adaptive regulation of the output currents of the DC motor load and stabilises the photovoltaic power generation. This is what we observed through the results obtained. We say that the proposed control provided the system with the stability of the output power of the GPV and also contributed to improving the speed of response to the consumption required by the load of the direct current motor and the quality of energy injected into the network.

REFERENCES

[1] S. Dhara, S. Jain, and V. Agarwal "A novel voltage-zone based power management scheme for PV- battery based standalone system," *2018 8th IEEE India Int. Conf. Power Electron.*, vol. 333, pp. 1–6, 2018.

[2] H. M. Hasanien, "Whale optimisation algorithm for automatic generation control of interconnected modern power systems including renewable energy sources," vol. 12, no. 3, 2017, doi: 10.1049/iet-gtd.2017.1005.

[3] A. Gheiratmand, R. Effatnejad, and M. Hedayati, "Technical and economic evaluation of hybrid wind / PV / battery systems for off-grid areas using HOMER software," vol. 7, no. 1, pp. 134–143, 2016, doi: 10.11591/ijpeds.v7.i1.pp134-143.

[4] B. V Rajanna, S. Lalitha, G. J. Rao, and S. K. Shrivastava, "Solar photovoltaic generators with MPPT and battery storage in microgrids," vol. 7, no. 3, pp. 701–712, 2016, doi: 10.11591/ijpeds.v7.i3.pp701-712.

[5] N. Aouchiche, "Meta-heuristic optimization algorithms based direct current and DC link voltage controllers for three-phase grid connected photovoltaic inverter," *Sol. Energy*, vol. 207, no. December 2019, pp. 683–692, 2020, doi: 10.1016/j.solener.2020.06.086.

[6] M. Lakshmi and S. Hemamalini, "Decoupled control of grid connected photovoltaic system using fractional order controller," *Ain Shams Eng. J.*, vol. 9, no. 4, pp. 927–937, 2018, doi: 10.1016/j.asej.2016.06.002.

[7] M. Farhat, M. Hussein, and A. M. Atallah, "Enhancement performance of a three phase grid connected photovoltaic system based on pi-genetic algorithm (pi-ga) controller," *2017 19th Int. Middle-East Power Syst. Conf. MEPCON 2017 - Proc.*, vol. 2018–Febru, no. December, pp. 145–151, 2018, doi: 10.1109/MEPCON.2017.8301177.

[8] S. Aatif, X. Yang, H. Hu, S. K. Maharjan, and Z. He, "Integration of PV and battery storage for catenary voltage regulation and stray current mitigation in MVDC railways," vol. 9, no. 3, pp. 585–594, 2021, doi: 10.35833/MPCE.2019.000155.

[9] S. Jadhav, N. Devdas, S. Nisar, and V. Bajpai, "Bidirectional DC-DC converter in solar PV system for battery charging application," *2018 Int. Conf. Smart City Emerg. Technol.*, pp. 1–4, doi: 10.1109/ICSCET.2018.8537391.

[10] M. Dehghani, M. Taghipour, G. B. Gharehpetian, and M. Abedi, "Optimized fuzzy controller for MPPT of grid-connected PV systems in rapidly," vol. 9, no. 2, pp. 376–383, 2021, doi: 10.35833/MPCE.2019.000086.

[11] T. Suntio *et al*., "Impedance-based interactions in grid-tied three-phase inverters in renewable energy applications," *Energies*, vol. 12, no. 3, 2019, doi: 10.3390/en12030464.

[12] R. Mahalakshmi and K. C. S. Thampatty, "Grid connected multilevel inverter for renewable energy applications," *Procedia Technol.*, vol. 21, pp. 636–642, 2015, doi: 10.1016/j.protcy.2015.10.076.

[13] P. Livinti, "Comparative study of a photovoltaic system connected to a three-phase grid by using PI or fuzzy logic controllers," *Sustainability*, vol. 13, no. 5, 2021, doi: 10.3390/su13052562.

[14] J. W. Kolar, T. Friedli, J. Rodriguez, and P. W. Wheeler, "Review of three-phase PWM AC – AC converter topologies," IEEE *Transactions on Industrial Electronics*, vol. 58, no. 11, pp. 4988–5006, 2011, doi: 10.1109/TIE.2011.2159353.

[15] V. Karthikeyan and R. Gupta, "Varying phase angle control in isolated bidirectional DC – DC converter for integrating battery storage and solar PV system in standalone mode," *IET Power Electronics*, vol. 10, no. 4, pp. 471–479, 2017, doi: 10.1049/iet-pel.2016.0162.

[16] A. Elgammal and T. Ramlal, "Adaptive voltage regulation control strategy in a stand-alone islanded DC microgrid based on distributed wind/photovoltaic/diesel/energy storage hybrid energy conversion system," vol. 5, no. 4, pp. 26–33, 2021, doi: 10.24018/ejece.2021.5.4.343.

[17] A. Tirupathi, K. Annamalai, and S. Veeramraju Tirumala, "A three-phase inverter circuit using half-bridge cells and T-NPC for medium-voltage applications," *Int. J. Circuit Theory Appl.*, vol. 48, no. 10, pp. 1744–1765, 2020, doi: 10.1002/cta.2833.

[18] N. Aouchiche, M. S. Aitcheikh, M. Becherif, and M. A. Ebrahim, "AI-based global MPPT for partial shaded grid connected PV plant via MFO approach," *Sol. Energy*, vol. 171, no. November 2017, pp. 593–603, 2018, doi: 10.1016/j.solener.2018.06.109.

[19] A. Mirzaei, M. Forooghi, A. Asghar, A. Hossein, and M. R. Riahi "Design and construction of a charge controller for stand-alone PV / battery hybrid system by using a new control strategy and power management," *Sol. Energy*, vol. 149, pp. 132–144, 2017, doi: 10.1016/j.solener.2017.03.046.

[20] E. H. M. Ndiaye, A. Ndiaye, M. Faye, and S. Gueye, "Intelligent control of a photovoltaic generator for charging and discharging battery using adaptive neuro-fuzzy inference system," vol. 2020, 2020, doi: 10.1155/2020/8649868.

[21] N. Chettibi and A. Mellit, "Intelligent control strategy for a grid connected PV / SOFC / BESS energy generation system Point of Common Coupling," *Energy*, vol. 147, pp. 239–262, 2018, doi: 10.1016/j.energy.2018.01.030.

[22] S. Bouallègue, J. Haggège, M. Ayadi, and M. Benrejeb, "PID-type fuzzy logic controller tuning based on particle swarm optimization," *Eng. Appl. Artif. Intell.*, vol. 25, no. 3, pp. 484–493, 2012, doi: 10.1016/j.engappai.2011.09.018.

[23] M. A. Sobhy, A. Y. Abdelaziz, H. M. Hasanien, and M. Ezzat, "Marine predators algorithm for load frequency control of modern interconnected power systems including renewable energy sources and energy storage units," *Ain Shams Eng. J.*, vol. 12, no. 4, 2021, doi: 10.1016/j.asej.2021.04.031.

[24] G. Boudechiche, M. Sarra, O. Aissa, J. Gaubert, B. Benlahbib, and A. Lashab, "Aalborg Universitet anti-windup FOPID-based DPC for SAPF interconnected to a PV system tuned using PSO Algorithm Boualam," *European Journal of Electrical Engineering*, vol. 22, no. 4-5, 2020, doi: 10.18280/ejee.224-503.
[25] H. Erdem and O. T. Altinoz, "Tuning of output scaling factor in PI-like fuzzy controllers for power converters using PSO," vol. 30, pp. 2677–2688, 2016, doi: 10.3233/IFS-152020.
[26] W. Z. Qiao and M. Mizumoto, "PID type fuzzy controller and parameters adaptive method," *Fuzzy Sets Syst.*, vol. 78, no. 1, pp. 23–35, 1996, doi: 10.1016/0165-0114(95)00115-8.
[27] E. Yazdani, A. Bagheri, B. Yazdani, S. Buyamin, and S. Nezamivand, "A new adjusting technique for PID type fuzzy logic controller using PSOSCALF optimization algorithm," *Appl. Soft Comput. J.*, vol. 85, p. 105822, 2019, doi: 10.1016/j.asoc.2019.105822.
[28] G. Boukhalfa, S. Belkacem, and A. Chikhi, "Direct torque control of dual star induction motor using a fuzzy-PSO hybrid approach," vol. 18, no. 1, pp. 74–89, 2022, doi: 10.1016/j.aci.2018.09.001.
[29] A. A. Firdaus, R. T. Yunardi, E. I. Agustin, S. D. N. Nahdliyah, and T. A. Nugroho, "An improved control for MPPT based on FL-PSo to minimize oscillation in photovoltaic system," *Int. J. Power Electron. Drive Syst.*, vol. 11, no. 2, pp. 1082–1087, 2020, doi: 10.11591/ijpeds.v11.i2.pp1082-1087.

BIOGRAPHIES OF AUTHORS

Benslimane Abdelkader was born in Béchar on octobre 21, 1971. He completed his university studies at the Faculty of Energetic physics, Tahri Mohamed Béchar University, Algeria, in 2016, and achieved an advanced rank in terms of merit.He has 20 years of experience in the field of electrical engineering, especially solar power plants in the field of telecommunications. He is currently working as a professor in physical measurements at the Higher Normal School of Béchar, Algeria. Benslimane Abdelkader has many international publications for research papers and many participations in international conferences. He can be contacted at email: slimane_kada@yahoo.com.

Abdelhak Merabti was born in Béchar on June 27, 1973. He completed his university studies at the Faculty of Exact Sciences, Tahri Mohamed Béchar University, Algeria, in 2017, and achieved an advanced rank in terms of merit. He has 22 years of teaching experience. He is currently working as a Professor at the Physics Department at the Higher Normal School of Béchar, Algeria. Abdelhak Merabti has many international publications for research papers and many participations in international conferences. He can be contacted at email: merabti73@yahoo.com.

Benslimane Yamina has done his research for Ph.D. degree in the field of Network and telecommunication from TAHRI Mohammed University in 2018, Algeria. He obtained a master's degree in computer science from the same university in 2012. His research interests include mobile networks, sensor networks, internet of things, smart energy and security. She can be contacted at email: yami.benslimane@gmail.com.